의학박사 학위논문

# Anticancer effect of BRD4 inhibitor in epithelial ovarian cancer

## 상피성 난소암에서 BRD4 inhibitor의 항암 효과

2023년 8월

서울대학교 대학원

의학과 산부인과학 전공

김 여 래

# Anticancer effect of BRD4 inhibitor in epithelial ovarian cancer

## 상피성 난소암에서 BRD4 inhibitor의 항암 효과

지도 교수 김 용 범

이 논문을 의학박사 학위논문으로 제출함
2023년 4월

서울대학교 대학원
의학과 산부인과학 전공
김 여 래

김여래의 의학박사 학위논문을 인준함
2023년 7월

위 원 장 (인)

부위원장 (인)

위 원 (인)

위 원 (인)

위 원 (인)

Abstract

# Anticancer effect of BRD4 inhibitor in epithelial ovarian cancer

Yeorae Kim

College of Medicine Obstetrics and Gynecology

The Graduate School

Seoul National University

Over the past decade, efforts have been made to develop bromodomain inhibitors as cancer treatments. Sub-pathways, particularly in ovarian cancer, affected by bromodomain-containing protein (BRD), remain unclear. We aimed to verify the antitumor effects of a new drug that can overcome OPT-0139-chemoresistance to treat ovarian cancer.

This *in vitro* and *in vivo* study used a mouse xenograft model of the human ovarian cancer cells SKOV3 and OVCAR3. Cells were treated with OPT-0139 (1-10 μM) ± cisplatin (10 μM) for 48 h. Cell viability and proliferation were assessed using MTT and ATP assays. Cell cycle arrest and apoptotic cell death were determined using flow cytometry. BRD4 and c-Myc expression and apoptosis-related molecules were detected using real-time PCR (RT-PCR) and Western blot. The xenograft tumors' growth rate, weight, and

immunohistochemistry were analyzed.
We confirmed the OPT-0139 effect and mechanism of action in epithelial ovarian cancer. OPT-0139 significantly reduced cell viability and proliferation and induced apoptotic cell death and cell cycle arrest. In a mouse xenograft model, significant changes in tumor growth, volume, weight, and BRD4-related gene expression were observed, indicating the antitumor effects of BRD4 inhibitors. Combination therapy with cisplatin promoted apoptotic cell death and suppressed tumor growth *in vitro* and *in vivo*.
Our results suggest a BRD4 inhibitor—OPT-0139—as a promising anticancer drug for ovarian cancer by inhibiting cell proliferation, decreasing cell viability, arresting cell cycle, and inducing apoptosis. OPT-0139, individually or in combination with cisplatin, may be a promising option for treating ovarian cancer.

Keywords: Ovarian cancer, BRD4, Anticancer effect
Student number: 2021-39572

# Table of contents

# List of figures and tables

Figures

# List of abbreviations

Abs: antibodies

BET: bromodomain and extra-terminal domain

Bcl-2: B-cell lymphoma-2

BRD: bromodomain-containing protein

BRDT: bromodomain testis-specific proteins

BAX: Bcl-2 associated X

CCK-8: Cell Counting Kit-8

c-Myc: Cellular myelocytomatosis oncogene

DMSO: dimethyl sulfoxide

EOC: epithelial ovarian cancer

FBS: fetal bovine serum

HIF-1a: hypoxia-inducible factor 1 subunit a

HOSEpic: human ovarian surface epithelial cell line

IACUC: Institutional Animal Care and Use Committee

IC50: half-maximal inhibitory concentration

OCT-4: octamer-binding transcription factor 4

NANOG: Nanog homeobox

p21: cyclin-dependent kinase inhibitor 1A

p27: cyclin-dependent kinase inhibitor 1B

PARP: poly ADP-ribose polymerase

PVDF: polyvinylidene fluoride

RT-PCR: real-time PCR

SD: standard deviation

VEGF: vascular endothelial growth factor

# Anticancer effect of BRD4 inhibitor in epithelial ovarian cancer

## 1. Introduction

Epithelial ovarian cancer (EOC) is the most aggressive gynecological cancer. It was reportedly the fifth leading cause of cancer-related deaths among women in the United States in 2018, with 21,410 newly diagnosed cases and 13,770 deaths by 2021 [1]. EOC is an aggressive malignancy; therefore, recurrence is common (almost 70–80%), and resistance to standard chemotherapy (platinum-based regimens) is frequent [2]. Few treatment options are available for patients with recurrent ovarian cancer after primary optimal debulking surgery and completion of front-line chemotherapy. Recurrence treatments include chemotherapy regimen changes and targeted therapies. Therefore, efforts have been made to overcome chemoresistance and decrease recurrence rates [2-4].

EOCs are characterized by high mortality and recurrence rates. This was the primary reason for developing this novel treatment option. One currently studied novel treatment option is targeted therapy, including poly ADP-ribose polymerase (PARP) inhibitor usage [5-7]. Promoting cell death by exploiting tumor DNA damage is the core mechanism of anticancer-targeted therapy. The epigenetic approach has recently gained attention, with bromodomain and extra-terminal domain (BET) as examples [8, 9]. BET proteins are epigenetic readers composed of four proteins: BRD2, BRD3, BRD4, and bromodomain testis-specific proteins (BRDT). Studies have revealed that BET proteins regulate cell

cycles and promote inflammatory cytokine production. Deregulation of BET proteins, particularly BRD4, has been studied in developing diverse diseases, especially cancer. BRD4 inhibitors have shown promising results in preclinical and clinical studies against various types of cancer, including leukemia, lymphoma, and solid tumors such as breast, lung, and prostate cancers [8–11].

However, the correlation between ovarian cancer treatment and BRD4 inhibitors remains unclear due to the heterogeneous carcinogenic characteristics of ovarian cancer, which differ from those of other cancers [12]. Despite the efforts to use bromodomain inhibitors as anticancer drugs, only a few have studied the correlation between BRD4 and ovarian cancer pathogenesis [13, 14]. Therefore, to overcome the challenges of treating ovarian cancer, we aimed to verify the antitumor effect of a novel drug, OPT–0139, that can overcome chemoresistance.

## 2. Materials and methods

### 2.1. Antibodies (Abs) and drugs

Dulbecco's modified Eagle's medium, nonessential amino acids, penicillin, sodium pyruvate, trypsin, and fetal bovine serum (FBS) were purchased from Gibco (Rockville, MD, USA). Anti–BRD4 (ab244221; mouse Ab; 1:1000) and anti–BCL–2 (ab692; mouse Ab; 1:1000) Abs were purchased from Abcam (Cambridge, USA). Anti–Cleaved Caspase–3 (9661; rabbit Ab; 1:1500), anti–Cleaved PARP (5625; rabbit Ab; 1:1000), and β–actin (3700; mouse Ab; 1:4000) Abs were purchased from Cell Signaling Technology (CST, MA, USA). OPT–0139 was obtained from ONCO pharmatech Inc. (Seongnam, Korea), and cisplatin were purchased from Sigma

Aldrich (St. Louis, MO, USA) and dissolved in dimethyl sulfoxide (DMSO) for *in vitro* studies and 0.9% saline for animal studies.

### *2.2. Cell culture*

Human ovarian cancer cell lines (SKOV3 and OVCAR3) were purchased from the American Type Culture Collection (VA, USA). An immortalized normal human ovarian surface epithelial cell line (HOSEpic) was obtained from ScienCell Research Laboratories, Inc. (Carlsbad, CA, USA). The cells were maintained in Roswell Park Memorial Institute-1640 culture (RPMI-1640; Gibco; Thermo Fisher Scientific, Inc., Carlsbad, CA, USA) supplemented with 10% (v/v) FBS, 100 mg/mL streptomycin, and 100 U/mL penicillin (P/S; Gibco; Thermo Fisher Scientific, Inc.) and incubated at 37°C, 5% $CO_2$.

### *2.3. Cell viability assay*

Cell viability was determined using PrestoBlue Cell Viability Reagent (Invitrogen, Carlsbad, CA, USA). Cells were seeded in 96-well plates in completed media 100 μL (containing 10% FBS and 1% P/S-supplemented media) per well and maintained overnight at 95% humidity and 5% $CO_2$. After incubating overnight, OPT-0139 was treated with 0–10 μM in 100 μL of completed media for 48 h. The final DMSO concentration in each well never exceeded 0.1%. The cells were incubated for 1 h with 10% PrestoBlue in the dark. Absorbance was measured at 540 nm using a plate reader and normalized to the cell number (absorbance/cell number). Statistical analyses were performed using GraphPad Prism version 9.4.1 for Windows. Significant values were considered at $p < 0.05$, and more significant values were considered at $p < 0.01$, compared with the

control.

*2.4. Cell proliferation assay*

Cell proliferation was determined using Cell Counting Kit-8 (CCK-8) Reagent (Dojindo Laboratories Co. Ltd., Tokyo, Japan). The cells were seeded into 96-well plates at $1 \times 10^4$ cells/well μL density and treated with different OPT-0139 concentrations (0, 0.01, 0.1, 0.5, 1, 5, and 10 μM) for 48 h. The CCK-8 assay was performed 48 h after OPT-0139 treatment. The serum-free medium was replaced, and 10 μL of CCK-8 was added to each well. After incubation at 37°C and 5% $CO_2$ for 1 h, the OD value was measured at 450 nm. Each measurement was performed in triplicate.

*2.5. Immunofluorescence staining*

Cells were seeded at $5\times10^4$ cells/well onto a 15 mm poly-L-lysine coated cover glass in a 6-well plate and incubated at 37°C for 24 h. The cells were fixed with 4% paraformaldehyde, permeabilized in 0.1% Triton X-100 for 15 min at RT, and washed thrice for 3 min with phosphate-buffered saline (PBS). The cells were blocked with 1% bovine serum albumin (Cat# A7030, Sigma Aldrich, St. Louis, MO, USA) for 60 min at room temperature. After washing thrice with PBS for 10 min, the samples were incubated with an anti-BRD4 monoclonal antibody overnight at 4°C. After the three 3-min washes with PBS, the cells were incubated with Alexa Fluor Plus 488 conjugated Goat anti-rabbit immunoglobulin G (1:1000, Cat# A32731, Thermo Fisher Scientific, Waltham, MA, USA) for 2 h at room temperature. Mitochondria were stained with MitoTracker Orange (1:5000, Cat# M7511, Thermo Fisher Scientific, Waltham, MA, USA) for 15 min at room temperature. Fluorescence-labeled

HOXB9 and mitochondria were observed and photographed using a fluorescence microscope.

*2.6. Caspase-3 activity*

Cells were seeded at $1\times10^4$ cells/well in white-walled 96 well plates for 24 h and treated with OPT-0139 in 0, 0.01, 0.1, 0.5, 1, 5, and 10 μM concentrations for 48 h. Treated cells were further incubated with 100 μL of Caspase-Glo 3/7 Reagent (Cat# G8090, Promega, Madison, WI, USA) at room temperature for 30 min. The Luminescence of each sample was measured using a luminometer (Molecular Devices). All data were expressed as percentages of the control.

*2.7. Annexin V FITC and propidium iodide (PI) apoptosis detection assay*

Annexin V and propidium iodide staining were performed using an annexin V FITC/PI apoptosis detection assay kit (Invitrogen, Carlsbad, CA, USA). Cells were seeded in 6-well plates at $5\times10^5$ cells/well. OPT-0139 was added at 0, 1, and 10 μM; cells were incubated further for 48 h. Cells were harvested using trypsinization, collected via centrifugation, washed once with 1 mL of PBS, stained according to the manufacturer's protocol, and analyzed using a flow cytometer (FACSCalibur, BD Bioscience, CA, USA).

*2.8. Cell cycle arrest*

Treated cell samples were washed with ice-cold PBS and fixed with 70% ethanol at −20°C overnight. The samples were then washed with PBS, resuspended in 0.5 mL of FxCycle™ PI/RNase

Staining Solution (Invitrogen) containing 50 μg/mL PI and 100 μg/mL RNase A, and incubated for 30 min at room temperature in the dark. The samples were analyzed using a FACSCalibur flow cytometer (BD Bioscience, CA, USA).

*2.9. Cell-derived mouse tumor xenografts model*

Forty BALB/c nude female mice (7 weeks old) were provided by ORIENT BIO Inc. (Seongnam, Korea). Mice were housed in a pathogen-free room at a controlled temperature (25 ± 2°C) and humidity (65 ± 5%) and alternating 12 h-light/-dark cycles. After acclimation for 1 week, 100 μL of Matrigel containing $5\times10^7$ SKOV3 cells were subcutaneously injected into the right flanks of BALB/c nude mice. We excluded the mice whose tumor size was less than 150 $mm^3$ four weeks after implantation. Mice with successful skin tumor formation were randomly divided into three groups (n = 10 for each group) as follows:

- Group 1: tumor control (implanted SKOV3 cells)
- Group 2: tumor cell implantation and intravenous low-dose OPT-0139 (5 mg/kg)
- Group 3: tumor cell implantation and intravenous high-dose OPT-0139 (20 mg/kg)

Tumor areas were measured once every 4 days and calculated as ([width (mm) × width (mm)] × length [mm])/2 using a Vernier caliper. OPT-0139 was dissolved in PBS and intravenously administered once every 3 days. For the continuous 4-week treatment, body weight was measured twice weekly. Mice were then euthanized, and the tumors were isolated. All animal experiments followed the guidelines of the Seoul National University Bundang Hospital Institutional Animal Care and Use

Committee (IACUC). Institutional Review Board statement: The IACUC of the Seoul National University Bundang Hospital approved the study (No. BA-2111-332-010-02) (approval date: November 26, 2021).

*2.10. Immunohistochemical staining*

Tumor tissues from cell-derived xenograft mice were deparaffinized, rehydrated, and washed twice with buffer. The slides were incubated in a Hydrogen Peroxide Block for 10 min and washed four times with the buffer to reduce nonspecific background staining due to endogenous peroxidases. Primary antibodies were added and incubated according to the manufacturer's instructions. The slides were then washed four times with the buffer. The slides were treated with a primary antibody enhancer, incubated for 20 min at room temperature, and washed four times with the buffer. Afterward, the HRP Polymer was applied to the slides, which were incubated for 30 min at room temperature and washed four times in buffer. Finally, they were incubated with hematoxylin as a chromogen and washed four times with deionized water.

*2.11. Quantitative real-time PCR analysis*

Total RNA was extracted from the isolated tumor samples using the TRIzol reagent (Invitrogen) according to the manufacturer's instructions. Equal quantities of DNA-free RNA were reverse transcribed to generate cDNA using GoScript™ Reverse Transcriptase (Promega). The real-time PCR was carried out in a 25 μL-reaction volume using 3 μL of a 1:10 cDNA dilution containing SYBR Green master mix (BioRad) and primers for PCR, BRD4, cyclin-dependent kinase inhibitor 1A (p21), cyclin-

dependent kinase inhibitor 1B (p27), MYC proto-oncogene, bHLH transcription factor (c-Myc), hypoxia-inducible factor 1 subunit alpha, vascular endothelial growth factor (VEGF), octamer-binding transcription factor 4 (OCT-4), Nanog homeobox (NANOG), b-cell lymphoma 2 (BCL-2), and Bcl-2 associated X (BAX). All PCRs were performed using a Qiagen Rotor-Gene Q real-time PCR system, and fluorescence threshold values (Ct) were calculated. Relative mRNA levels were assessed via standardization with 18s rRNA. The results were expressed as a fold difference in gene expression.

*2.12. Protein preparation and western blot*

The cells were treated with indicated drugs for 48 h; treated cells were harvested and lysed in a lysis buffer (50 mM Tris-HCl, 1% NP40, 150 mM NaCl, 1 mM EDTA, and 1 mM PMSF) for 30 min at 4°C. Total cell extracts were separated using 12% SDS-PAGE and transferred onto polyvinylidene fluoride (PVDF) membranes. Membranes were blocked with 5% skimmed milk and incubated with primary antibodies diluted in the blocking solution. The signals were visualized using the chemiluminescent substrate method and Super Signal West Pico kit (Pierce, Thermo Fisher Scientific). β-actin was used as an internal control to normalize loading.

*2.13. Immunoblot analysis*

Cell monolayers were washed once with ice-cold saline and lysed by adding PROPREP (50 mM Tris-HCl [pH 8.0], 150 mM NaCl, 1% Triton X-100, 0.5% sodium deoxycholate, and 0.1% SDS) and protease inhibitors (INTRON Biotechnology). They were incubated for 1 h at 4°C with gentle agitation, harvested with a cell scraper,

and transferred to a 1.5 mL tube. The lysate was then centrifuged at 12000 ×*g* for 10 min at 4°C, and the supernatants were recovered and stored at −80°C. Protein concentrations were determined using the bicinchoninic acid protein assay (Pierce, Thermo Fisher Scientific). Total cell extracts were separated using 12% SDS−PAGE and transferred onto PVDF membranes. The membranes were blocked with 5% skimmed milk and incubated with primary antibodies diluted in a blocking solution. Signals were visualized using the chemiluminescent substrate method and Super Signal West Pico kit (Pierce, Thermo Fisher Scientific). β−actin was used as an internal control to normalize loading.

### *2.14. Statistical analysis*

Each experiment was performed in triplicate and repeated at least thrice. Statistical values are expressed as mean ± Standard Deviation (SD). The Mann–Whitney U test was performed to evaluate statistical differences. All statistical tests were two−sided, and a p−value of < 0.05 was considered significant in all cases. P−values less than 0.5 are denoted by *, < 0.01 by **, and < 0.001 by ***. GraphPad Prism (GraphPad Software, 9.4.1) was used for statistical analyses.

## 3. Results

### *3.1. BRD4 overexpression in ovarian cancer cells and half−maximal inhibitory concentration of OPT−0139*

To evaluate BRD4 expression in ovarian cancer cell lines, we used SKOV3, A2780, OVCAR3, and CAOV3 cell lines. The experiments were conducted with high−grade serous ovarian adenocarcinoma cell lines SKOV3 and OVCAR3 because of their high BRD4

expression levels. HOSEpic was used as a control group. Western blot analysis was performed to compare BRD4 expression in each cell line, and relative mRNA levels were measured by quantitative real-time PCR. BRD4 expression was higher in SKOV3 and OVCAR3 cells than in the other cell lines (Figures 1A, B).

The half-maximal inhibitory concentration (IC50) of OPT-0139 was evaluated to determine its potency to reduce ovarian cancer cell line viability. SKOV3 and OVCAR3 cells were treated with 1 nM–100 μM of OPT-0139 for 48 h (Figure 1C, D). Cell viability was measured after 48 h; the IC50 value for the drug were 1.568 and 1.823 μM in the SKOV3 and OVCAR3 cell lines, respectively.

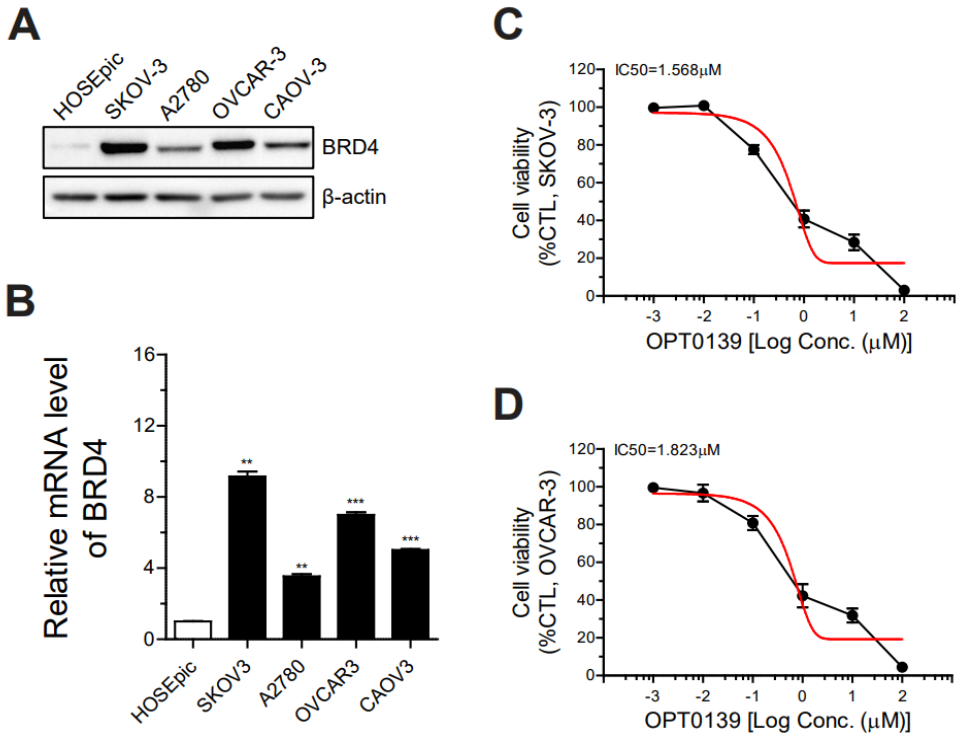


Figure 1. BRD4 expression in various ovarian cancer cell lines, SKOV3, A2780, OVCAR3, CAOV3, and HOSEpic. (A) Western blots and (B) relative mRNA levels of each cell line were examined. (** $p$ <0.01, *** $p$ <0.001 compared to control group). (C, D) To measure the IC50 value of OPT-0139, ,SKOV3 and OVCAR3 cells were treated with OPT-0139 at a

concentration of 1 nM to 100 μM for 48 h. Abbreviations: BRD4, Bromodomain-containing protein 4; HOSEpic, Human Ovarian Surface Epithelial Cells; IC50, half-maximal dose.

*3.2. OPT-0139's inhibitory effect on cell survival and proliferation*

To explore the inhibitory effect of OPT-0139 on cell viability and proliferation, the Presto Blue assay and CCK-8 assay were performed. Based on the IC50 value of OPT-0139, the effective concentrations of the drug were 0, 0.01, 0.1, 0.5, 1, 5, and 10 μM. SKOV3 and OVCAR3 cells were treated with OPT-0139 at each concentration for 48 h to determine cell viability and proliferation (Figure 2A, B). Regarding cell viability, PrestoBlue reagent based on the MTT assay was used; for proliferation, the CCK-8 assay was dose-dependent with OPT-0139. Consequently, cell viability decreased from 0.1 μM of OPT-0139 in SKOV3 and OVCAR3 cells (Figure 2A). Moreover, cell proliferation decreased dose-dependently from 0.5 μM (Figure 2B). OPT-0139 caused a dose-dependent decrease in ovarian cancer cell viability and proliferation. In addition, immunocytochemistry was used to identify cell structure change and BRD4 expression. SKOV3 cells were treated with OPT-0139, and green fluorescence indicated BRD4, whereas red indicated mitochondrial staining to confirm the cell shape (Figure 2C). As shown in Figure 2C, treatment with OPT-0139 decreased BRD4 expression in the ovarian cancer cell lines.

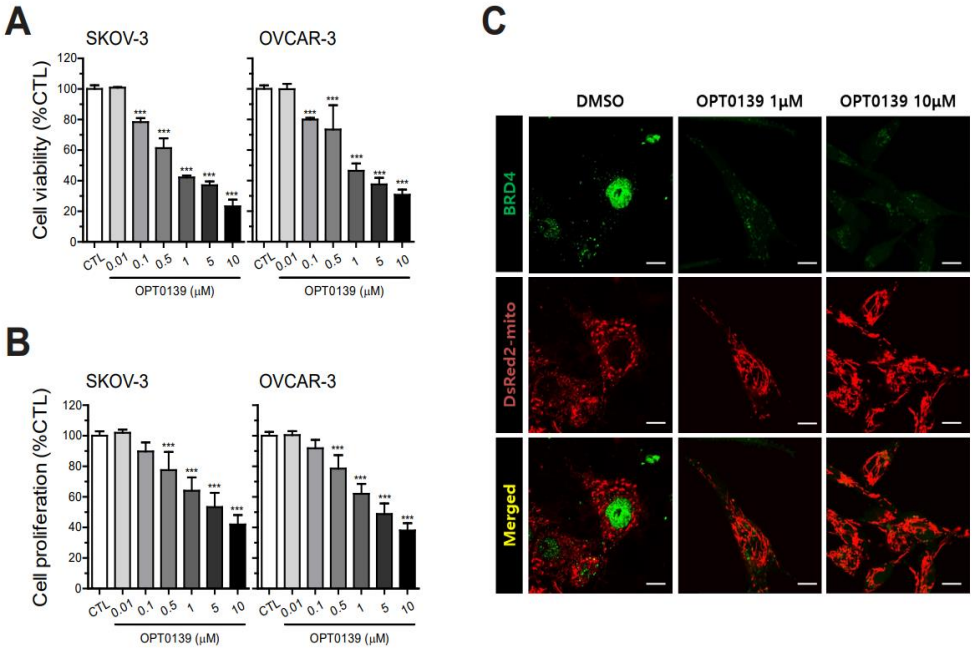


Figure 2. Inhibition of cancer cell survival and proliferation by OPT-0139: SKOV3 and OVCAR3 were treated with OPT-0139 for 48 h at each concentration to determine (A) cell viability and (B) cell proliferation, respectively, PrestoBlue reagent based on MTT assay and CCK-8 assay were used (*** $p$ <0.001 compared to control group). (C) Immunocytochemistry in SKOV3. Green fluorescence: BRD4, red fluorescence: mitochondria. Abbreviations: BRD4, bromodomain-containing protein 4.

### *3.3. OPT-0139's induction of apoptotic cell death*

To identify the correlation between BRD4 inhibitor and apoptotic cell death induction, annexin V and PI staining was performed on SKOV3 and OVCAR3 cell lines with OPT-0139 incubation for 48 h. Flow cytometry analysis of annexin V-PI staining showed that the apoptotic cell count, especially early apoptosis, increased dose-dependently in SKOV3 and OVCAR3 upon OPT-0139 treatment. The quantitative analysis illustrates that SKOV3 and OVCAR3 significantly increased apoptosis depending on OPT-0139 concentration. (*** $p$ <0.001) (Figure 3A).

A caspase-3 activity assay showed that OPT-0139 significantly

induced caspase-3 activity in a concentration-dependent manner (Figure 3B). Western blot analysis was performed to evaluate apoptotic signaling protein expression. Western blot analysis showed that OPT-0139 decreased the anti-apoptotic molecule—Bcl-2. Contrarily, the pro-apoptotic molecules' expression of cleaved caspase-3 and PARP increased (Figure 3C). Thus, these results demonstrated that the BRD4 inhibitor activates the apoptosis signaling pathway and induces apoptosis.

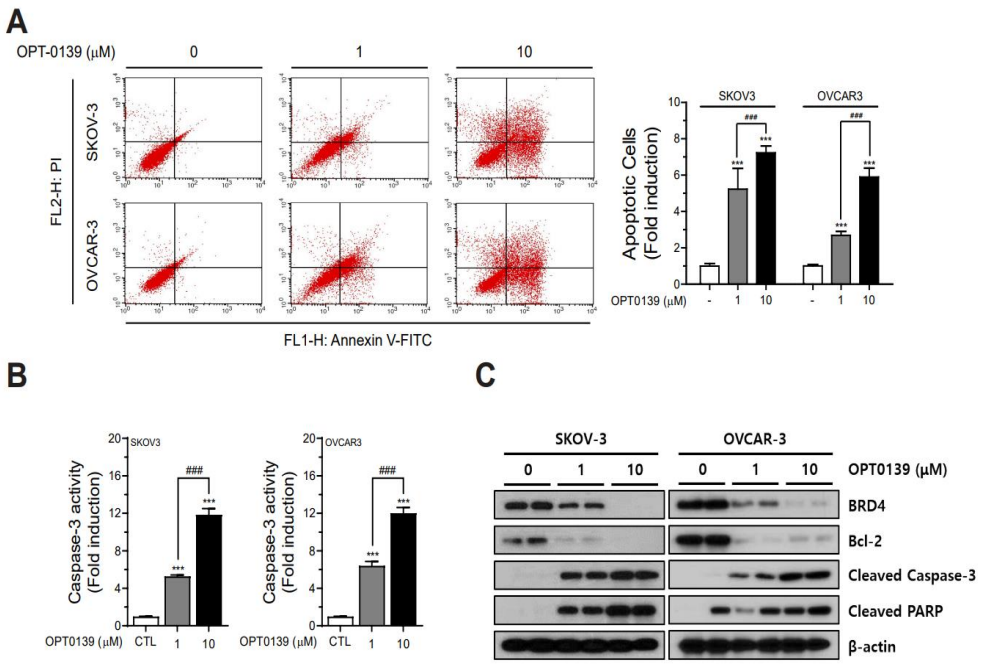


Figure 3. Induction of apoptotic cell death by OPT-0139: The SKOV3 and OVCAR3 cells were treated with the indicated doses of OPT-0139 for 48 h, and then (A) apoptosis and (B) Caspase-3 activity analysis of SKOV3 and OVCAR3 cells were conducted following OPT-0139 treatment (*** p <0.001 compared to control group, ### p <0.001 compared to experimental groups); (C) Western blot. Abbreviations: BRD4, Bromodomain-containing protein 4; Bcl-2, B-cell lymphoma-2

### *3.4. OPT-0139's induction of cell cycle arrest*

To explore whether OPT-0139 causes cell cycle arrest in ovarian

cancer cells, SKOV3 and OVCAR3 cells were treated with OPT-0139 and cell cycle analyses were done by flow cytometry. OPT-0139 induced G1 phase arrest in both ovarian cancer cell lines. It decreased the G1 phase cell count and increased the G2/M phase cell count (Figure 4A, B). RT-PCR was performed to understand the cell cycle arrest pathway. In both ovarian cancer cell lines, SKOV3 and OVCAR3, BRD4 expression decreased, whereas CDKN1A (p21) gene expression and degradation of the cell cycle inhibitor CDKN1B/p27KIP1 (p27) increased in a dose-dependent manner. The expression of c-Myc also decreased (Figure 4C).

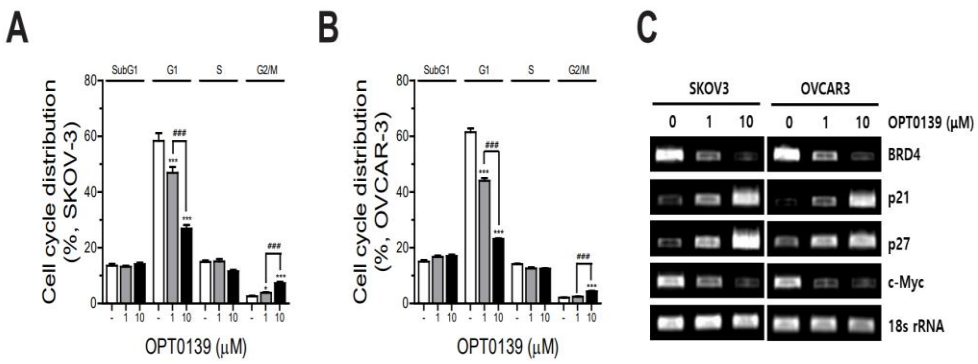


Figure 4 Cell cycle arrest induction by OPT-0139: OPT-0139 effects cell cycle phase distribution of (A) SKOV3 and (B) OVCAR3 cells (*** p <0.001 compared to control group, ### p <0.001 compared to experimental groups); (C) RT-PCR analysis for understanding the cell cycle arrest pathway. Abbreviations: p21, CDKN1A; p27, CDKN1B/p27KIP1; c-Myc, MYC proto-oncogene; bHLH, transcription factor

### *3.5. OPT-0139's inhibition of tumorigenesis in a mouse xenograft model*

A xenograft mouse model was established to determine the potential therapeutic effect of OPT-0139 on tumor growth, and tumor volumes were measured every 3 days. We examined the

effects of OPT-0139, a single treatment, on the tumor growth of SKOV3 cells *in vivo*, and the SKOV3 cells are highly tumorigenic in nude mice. The female BALB/c nude mice (8 weeks old) were used as an animal model to prepare the mouse xenograft model. Each mouse was inoculated subcutaneously with 100 μL of Matrigel and human ovarian cancer SKOV3 cells ($5X10^7$). We excluded the mice whose tumor size was <150 $mm^3$. Mice were divided into 3 groups (n = 10) 30 days after inoculation and matched for tumor volume. Mice groups were treated with intravenous injection of OPT-0139 and were sacrificed after 4 weeks of treatment, and tumor tissues were collected. We monitored the tumor growth rate and body weight for each mouse group, and the OPT-0139 single treatments notably reduced the tumor growth rate in mice compared to that in control groups (Figure 5A). BRD4 expressions were detected in mouse xenograft tumors using immunohistochemistry (Figure 5C). Furthermore, the single treatment of OPT-0139 significantly suppressed the final tumor weight and volume in a dose-dependent manner (Figure 5D). However, no impact on body weight was found in either of the mouse groups (Figure 5B, D). These *in vivo* data strongly suggest that OPT-0139 single treatment significantly suppressed tumorigenesis in a mouse tumor xenograft model.

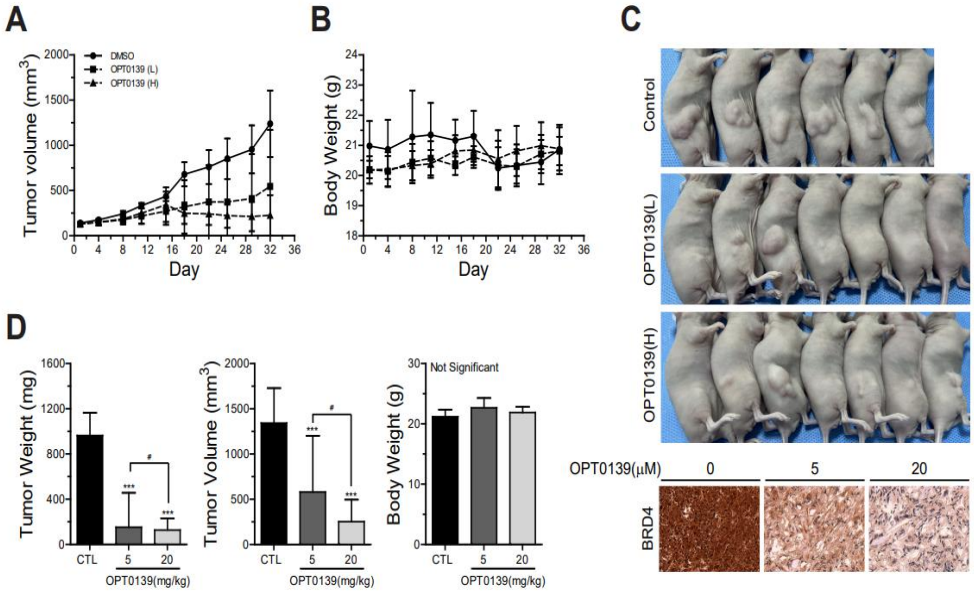


Figure 5. Anticancer effect of OPT-0139 in mouse xenograft models: (A) Tumor growth rate with OPT 0139 low-dose and high-dose injection in SKOV3 injected mouse models. For 4 weeks, the tumor volume is measured after the implantation of SKOV3 cells. The two-tailed Student's t-test was used to analyze the differences between the groups. (B) Body weight of xenograft mice; (C) each group of representative mice's gross tumors before harvest and BRD4 immunohistochemical staining analysis in the tumors of SKOV3 cells (*** $p < 0.001$ compared to control group, # $p < 0.05$ compared to experimental groups).

### *3.6. OPT-0139 alters hypoxia signaling, angiogenesis, cancer stemness, and apoptosis gene expression levels in tumors*

To assess whether OPT-0139 affects mRNA expression of hypoxia signaling, angiogenesis, cancer stemness, and apoptosis markers, total RNA was isolated from control, OPT-0139 5 or 20 mg/kg-injected mouse tumor and analyzed by semi-quantitative real-time-PCR. The mRNA expression levels of BRD4 and hypoxia signaling genes were markedly decreased (BRD4, ~50 and ~70%, Hif-1α, ~40 and ~70, respectively) in the OPT-0139 5 or 20 mg/kg-injected groups (Figure 6A, B). Furthermore, the mRNA

expression levels of VEGF (angiogenesis), Oct-4, and Nanog (cancer stemness) were suppressed by ~50% for OPT-0139 5 or 20 mg/kg-injected group (Figure 6C-E). Additionally, mRNA expression levels of Bcl-2 (anti-apoptosis) were decreased by 50 and 70% (Figure 6F), and the mRNA expression levels of BAX (anti-Bcl-2) were increased by ~2.5 fold for the OPT-0139 5 or 20 mg/kg-injected groups, respectively (Figure 6G). A significant difference was observed in every feature when comparing the differences between the control, low-dose, and high-dose groups. Even though the *p*-value was less than 0.5 between low-dose and high-dose groups, they showed a statistically significant difference (Figure 6A-G). These results indicate the inhibition or activation effects of OPT-0139 on BRD4, hypoxia signaling, and tumor progression.

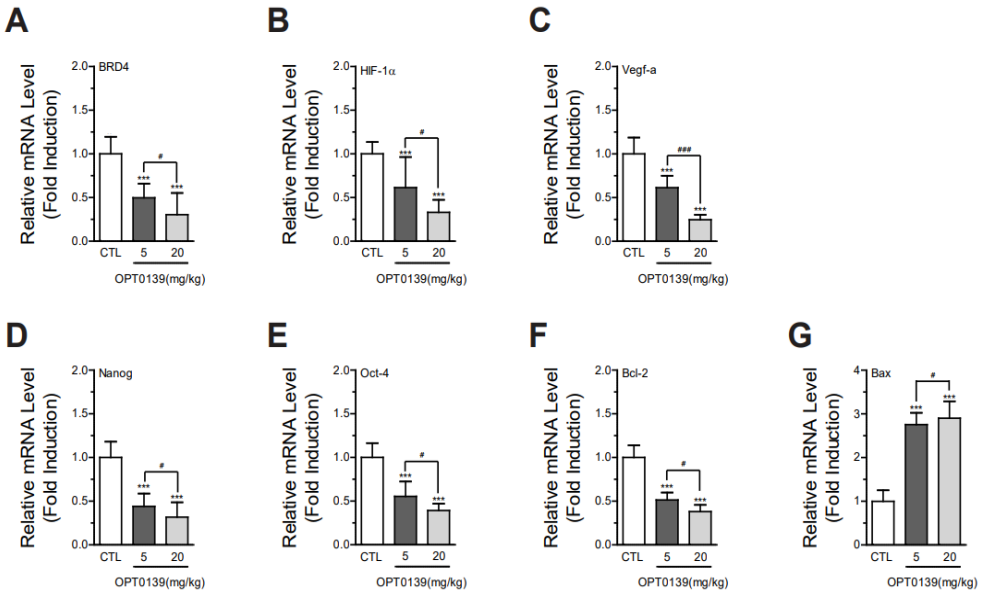


Figure 6. Relative mRNA level measurement: (A) BRD4, Bromodomain-containing protein; (B) HIF-1a, Hypoxia-inducible factor; (C) Bcl-2, b-cell lymphoma 2; (D) BAX, Bcl-2 associated X; (E) VEGF-a, vascular endothelial growth factor; (F) Nanog, Nanog homeobox; (G) Oct-4, octamer-binding transcription factor 4 (*** p <0.001 compared to control group, # p <0.05, ### p <0.001 compared to experimental groups).

*3.7. Combining OPT-0139 with cisplatin in ovarian cancer cells*

To investigate the possible synergistic impact of OPT-0139 with cisplatin in ovarian cancer cells, SKO3 and OVCAR3 cell lines were treated with 0.1 μM OPT-0139 with or without 10 μM cisplatin. The combination of OPT-0139 with cisplatin showed that cell viability was reduced by about half in both cell lines compared to using either agent (Figure 7A). Caspase-3 activity was performed with the same setting of 0.1 μM OPT-0139 with or without 10 μM cisplatin in two cell lines. The result showed that the combined use of OPT-0139 and cisplatin increased the activity of caspase-3 by 4–5 times compared to the groups with independent use of each agent (Figure 7B). Cell viability and caspase-3 activity showed statistical differences between the four groups—control vs. OPT-0139 alone vs. cisplatin alone vs. combination group (Figure 7A, B). Western blot analysis was performed with OPT-0139 and cisplatin combination setting to compare the effects of monotherapy of each drug and combination therapy. On a protein level, no significant differences could be observed when cell lines were treated with OPT-0139 and cisplatin alone. However, when both drugs were combined, apoptosis-related molecules' expression showed the same trend but with a more pronounced effect. Expression of the anti-apoptotic molecule—Bcl-2—decreased, and expression of pro-apoptotic molecules—BAX, cleaved caspase-3, and PARP—increased (Figure 7C).

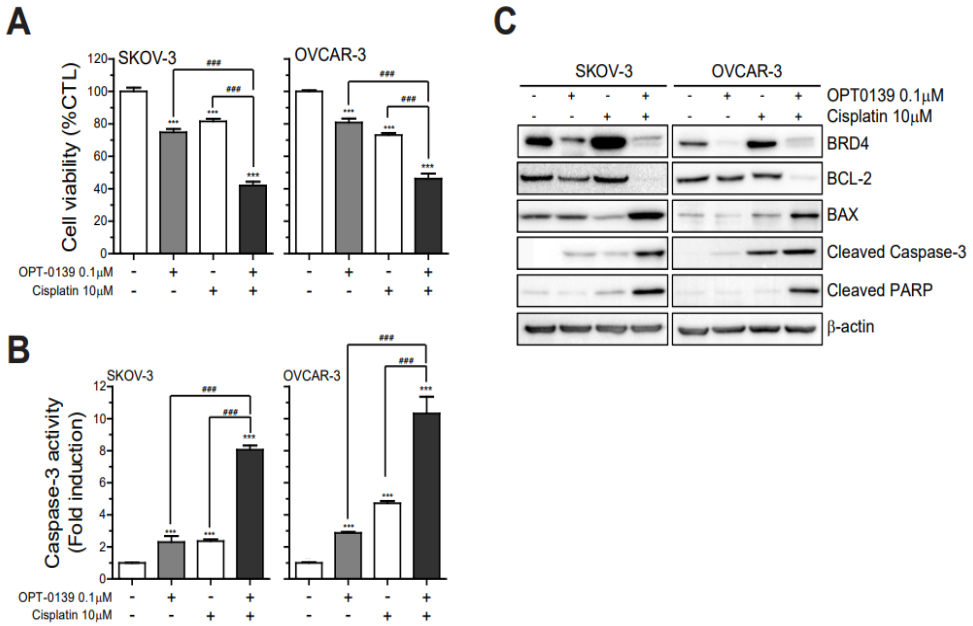


Figure 7. Additive effect of combining OPT-0139 with cisplatin in ovarian cancer cell: (A) Cell viability, (B) Caspase-3 activity, (C) Western blot. Abbreviations: BRD4, Bromodomain-containing protein 4; Bcl-2, b-cell lymphoma 2; BAX, Bcl-2 associated X; Cleaved PARP, Cleaved poly ADP-ribose polymerase (*** p <0.001 compared to control group, ### p <0.001 compared to experimental groups).

### *3.8. Combining OPT-0139 with cisplatin in a mouse xenograft model*

Based on the results of Figure 5, we validated the additive effect of combining OPT-0139 with cisplatin in a mouse xenograft model using SKOV3 cells. Four experimental settings were created: DMSO as a control group, OPT-0139 as a BRD4 inhibitor group, cisplatin as a chemotherapy group, and OPT-0139 as a cisplatin combination group. Compared to cisplatin alone, the tumor growth rate was significantly reduced when OPT-0139 was given in combination with cisplatin (Figure 8A). Tumor weight was measured in isolation from mice. Compared to the cisplatin alone group, the combination

of OPT-0139 reduced tumor weight by approximately 90% and tumor volume by approximately 80% (Figure 8C, D). Statistical differences between the monotherapy and combination groups of OPT-0139 and cisplatin are shown (Figure 8C-E). In addition, the body weights of all mice did not decrease when measured to check for side effects (Figure 8B, E).

To determine if OPT-0139–cisplatin combination treatment alters the expression level of BRD4, hypoxia signaling, angiogenesis, cancer stemness, and apoptosis marker genes, total RNA was isolated from the control, OPT-0139, cisplatin, OPT-0139/cisplatin-injected mouse tumor, and then analyzed by semi-quantitative real-time PCR. The expression level of BRD4 and hypoxia signaling genes were significantly decreased (BRD4, ~35 and ~20%; Hif-1α, ~55 and ~60%), respectively, in OPT-0139- or OPT-0139/cisplatin-injected groups (Figure 9A, B), but no significant changes were observed in expression levels in the cisplatin-injected group. Expression levels of VEGF (~50% and ~80%), Nanog (~40% and ~60%), and Oct-4 (~40% and ~45%) were suppressed in the OPT-0139 or OPT-0139/cisplatin-injected group (Figure 9C-E). Furthermore, mRNA expression levels of Bcl-2 were reduced by ~55 and ~70% (Figure 9F), and the mRNA expression levels of BAX were induced by ~2.5 and ~2.0 fold in OPT-0139 or OPT-0139/cisplatin-injected groups, respectively (Figure 9G). Every feature showed statistically significant differences ($p$-value $< 0.001$) (Figure 9A-G). Our results revealed that OPT-0139 has the potential to be developed as an effective therapy to overcome ovarian cancer.

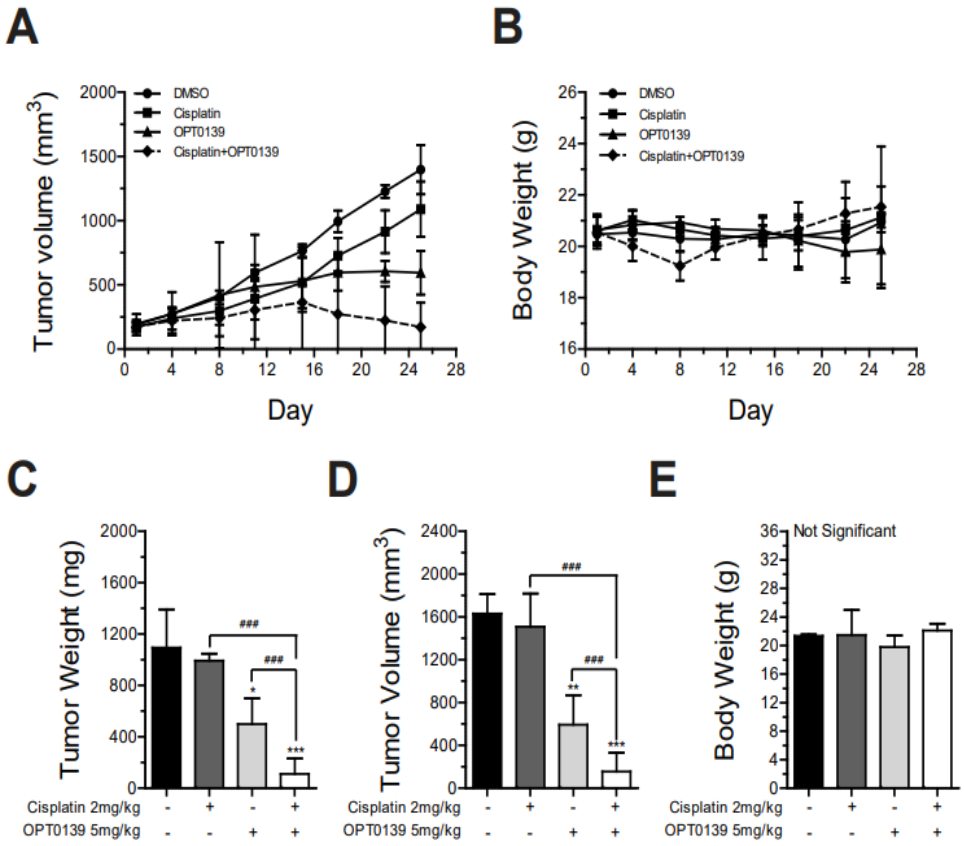


Figure 8. Additive effect of combining OPT-0139 with cisplatin in mouse xenograft models: mice were injected with cisplatin 2 mg/kg (intravenous) thrice a week. (A) Calculated tumor volume (● DMSO, ■ Cisplatin, ▲ OPT-0139, ◆ Cisplatin and OPT-0139 combination), (B) Body weight (● DMSO, ■ Cisplatin, ▲ OPT-0139, ◆ Cisplatin and OPT-0139 combination), (C) Tumor weight of isolated tumors from mice, (D) Tumor volume of isolated tumors from mice, (E) Body weight (* $p < 0.05$, ** $p < 0.01$, *** $p < 0.001$ compared to control group, ### $p < 0.001$ compared to experimental groups, N.S., not significant)

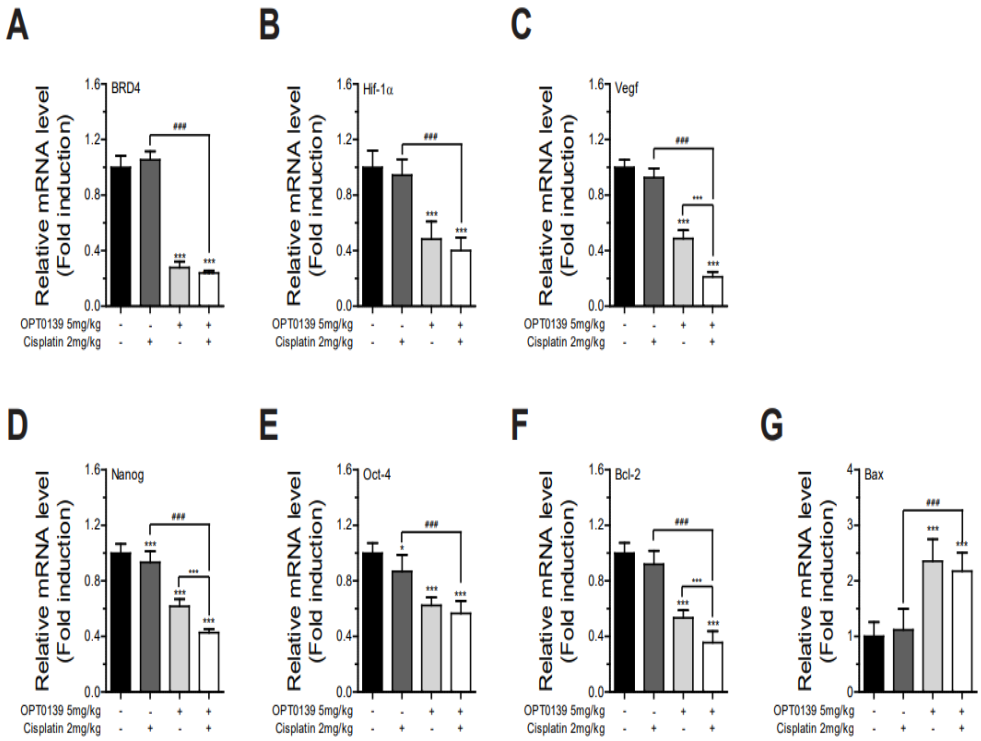


Figure 9. Relative mRNA levels between the control, cisplatin only, OPT-0139 only, and OPT-0139 and cisplatin combination groups: (A) BRD4, Bromodomain-containing protein; (B) HIF-1a, Hypoxia-inducible factor; (C) Bcl-2, b-cell lymphoma 2; (D) BAX, Bcl-2 associated X; (E) VEGF-a, vascular endothelial growth factor; (F) Nanog, Nanog homeobox; (G) Oct-4, octamer-binding transcription factor 4 (* p <0.05, *** p <0.001 compared to control group, ### p <0.001 compared to experimental groups).

## 4. Discussion

In the present study, we demonstrated an anticancer effect of the novel BRD4 inhibitor OPT-0139 in combination with the conventional cytotoxic agent cisplatin *in vitro* and *in vivo*. The laboratory findings were conducted with two ovarian cancer cell lines, SKOV3 and OVCAR3, and mouse xenograft models. We observed inhibition of cell survival and proliferation and induction of cell cycle arrest and apoptosis in the OPT-0139 and cisplatin groups. Our key findings suggest that OPT-0139 induces several anticancer effects, such as cell viability decrease and induction of apoptosis, independently and in combination with cisplatin.

BRD4 is overexpressed in various cancer cells, such as breast, colorectal, prostate, and gastric [15-18]. The small molecule BRD4 leads to dysregulated gene expression and promotion of cancer cell survival and proliferation. BRD4 inhibitors typically work by competitively binding to the bromodomain of BRD4, preventing its interaction with acetylated histones and other transcriptional co-factors [8, 9]. OPT-0139 also acts as a competitive binding monovalent molecule. This disrupts the normal transcriptional machinery, leading to downregulating oncogenes and upregulating tumor suppressor genes [8, 9, 19]. BRD4 inhibitors can also cause cell cycle arrest and induce apoptosis in cancer cells, further inhibiting their proliferation [8, 9, 19].

HIF-1a is one of the genes regulated by BRD4. Since HIF-1a is a transcription factor that regulates the expression of numerous genes involved in hypoxia responses, inhibiting its stability or activity can lead to reduced expression of HIF-1a target genes. This includes genes involved in angiogenesis, glycolysis, and other adaptive responses to low oxygen levels [20, 21]. HIF-1a and c-

Myc expression are correlated with cell cycle arrest and cell proliferation [22]. In ovarian cancer, c-Myc is overexpressed [23]. BRD4 is unevenly distributed within cancer cells, with higher concentrations observed of certain important oncogenes, such as c-Myc. It then promotes the activation of these genes, leading to increased cell growth [24-26]. Our study agent, OPT-0139, is designed to induce anticancer effects by interfering with HIF-1a signaling by inhibiting BRD4. And then, HIF-1a downregulated important cell cycle genes, such as c-Myc. We confirmed the signaling pathway with HIF-1a and c-Myc using RT-PCR (Figure 4C, 6, 9).

Inducing cell proliferation by promoting the transition from G1 to S phase during cell cycle progression is one of the most characteristic functions of c-Myc, a feature associated with its pro-tumor activity. Several mechanisms account for this, including repression of the CDKN2B (p15) and CDKN1A (p21) genes and degradation of the cell cycle inhibitor CDKN1B/p27KIP1 (p27) [27]. p21 and p27 act as universal inhibitors of Cyclin-dependent kinases (CDKs) by inhibiting various CDK-cyclin complexes [28, 29]. In ovarian cancer, the expression of these two proteins is associated with survival [30]. RT-PCR of the proteins involved was performed to determine if they induced cell cycle arrest, and it was found that p21 and 27 expressions increased in a concentration-dependent manner after OPT-0139 treatment, while c-Myc expression decreased (Figure 4C). By identifying these proteins, we were able to predict the pathway indirectly.

Few studies have attempted to adapt BRD4 inhibitors to treat ovarian cancer cells [13, 14, 31-33], and most of them have focused on the relationship between PARP inhibitors and BET

inhibitors or the correlation between BRD4 expression and basic function in ovarian cancer [14, 31, 32]. The heterogeneity of ovarian cancer is one of the reasons why, despite several studies, there has not been a game-changer in its treatment. Ovarian cancer carcinogenesis is heterogeneous and differs from other cancers. Its complexity makes treatment difficult, and the recurrence rate is high [12, 13]. Therefore, novel treatment options are needed, and epigenetic approaches have emerged. Among epigenetic anticancer drugs, BRD4 inhibitors have received attention owing to their various functions, such as decreased cell viability, cell proliferation, and apoptosis induction [8, 34]. While there is a lack of extensive data regarding the impact of BRD4 inhibitors on ovarian cancer in the existing literature, our research aligns with the outcomes of previous studies [13].

Our data are clinically relevant as we have revealed the possibility of overcoming the limitations of ovarian cancer treatment and the additive effect of a BRD4 inhibitor with the standard anticancer cisplatin. However, this study had some limitations in using mouse heterotopic xenograft models.

In Figure 7, the results showed a relatively poor response to cisplatin in the SKOV3 cell line (Figure 7A, C); this result was unexpected since we did not use a platinum-resistant SKOV3 cell line. The recent doubts raised about the histological derivation of SKOV3 cells pose difficulties in extending the conclusions of this study [35]. It is unclear whether this result is a characteristic of the SKOV3 cell line or the heterotopic xenograft mouse model used in this experiment or due to the concentration of cisplatin used. In addition, there have been multiple suggestions about the IC50 of cisplatin in the SKOV3 cell line. Thus, it is advisable to interpret the

results of the experiments performed on the SKOV3 cell line cautiously and plan any subsequent experiments with these results in mind [36, 37].

The subcutaneous model can easily evaluate subcutaneous tumor masses and is easy for tumor growth monitoring[38]. However, most ovarian cancer cells in patients grow in the abdominal cavity and rarely metastasize to the subcutaneous tissues. Since intraperitoneal or orthotopic models more reflect the tumor microenvironment than subcutaneous models, we can cautiously infer that cisplatin chemotherapy might not be as effective as expected in the subcutaneous SKOV3 tumor models[38].

In this study, we confirmed the tendency of the drug (OPT-0139) to exhibit additive effects with cisplatin. Compared to OPT-0139 used alone, the combination of cisplatin and OPT-0139 displayed a greater decrease in BRD4 expression and tumor cell viability; cell viability decreased by about 40% with the use of cisplatin alone and by almost 60% with the combined use of OPT-0139 and cisplatin (Figure 7A). Changes in the expression of apoptosis signaling molecules, including decreased cell viability and caspase-3 activity, suggest that the combination therapy has an additive effect.

In summary, our study has validated a new BRD4 inhibitor, OPT-0139, as a promising anticancer agent for ovarian cancer treatment. Furthermore, once validated in preclinical trials, initial assessments showed that treatment effectiveness could be improved when combined with conventional cytotoxic agents, offering hope to poor responders to current treatments. Further research into the role of BRD4 inhibitors in inhibiting metastasis in ovarian cancer, as shown in breast cancer, would help treat ovarian cancer [8].

## Bibliography

[1] Siegel RL, Miller KD, Fuchs HE, Jemal A. Cancer Statistics. CA Cancer J Clin. 2021;71:7-33.
[2] Garzon S, Lagana AS, Casarin J, Raffaelli R, Cromi A, Franchi M, et al. Secondary and tertiary ovarian cancer recurrence: what is the best management? Gland Surg. 2020;9:1118-29.
[3] Pignata S, C Cecere S, Du Bois A, Harter P, Heitz F. Treatment of recurrent ovarian cancer. Ann Oncol. 2017;28:viii51-viii6.
[4] Petersen S, Wilson AJ, Hirst J, Roby KF, Fadare O, Crispens MA, et al. CCNE1 and BRD4 co-amplification in high-grade serous ovarian cancer is associated with poor clinical outcomes. Gynecol Oncol. 2020;157:405-10.
[5] Smith M, Pothuri B. Appropriate Selection of PARP Inhibitors in Ovarian Cancer. Curr Treat Options Oncol. 2022;23:887-903.
[6] Cortez AJ, Tudrej P, Kujawa KA, Lisowska KM. Advances in ovarian cancer therapy. Cancer Chemother Pharmacol. 2018;81:17-38.
[7] Orr B, Edwards RP. Diagnosis and Treatment of Ovarian Cancer. Hematol Oncol Clin North Am. 2018;32:943-64.
[8] Duan Y, Guan Y, Qin W, Zhai X, Yu B, Liu H. Targeting Brd4 for cancer therapy: inhibitors and degraders. Medchemcomm. 2018;9:1779-802.
[9] Donati B, Lorenzini E, Ciarrocchi A. BRD4 and Cancer: going beyond transcriptional regulation. Mol Cancer. 2018;17:164.
[10] Sun Y, Han J, Wang Z, Li X, Sun Y, Hu Z. Safety and Efficacy of Bromodomain and Extra-Terminal Inhibitors for the Treatment of Hematological Malignancies and Solid Tumors: A Systematic Study of Clinical Trials. Front Pharmacol. 2020;11:621093.
[11] Asangani IA, Dommeti VL, Wang X, Malik R, Cieslik M, Yang R, et al. Therapeutic targeting of BET bromodomain proteins in castration-resistant prostate cancer. Nature. 2014;510:278-82.
[12] Gee ME, Faraahi Z, McCormick A, Edmondson RJ. DNA damage repair in ovarian cancer: unlocking the heterogeneity. J Ovarian Res. 2018;11:50.
[13] Drumond-Bock AL, Bieniasz M. The role of distinct BRD4 isoforms and their contribution to high-grade serous ovarian carcinoma pathogenesis. Mol Cancer. 2021;20:145.
[14] Huang Y, Liu C, You L, Li X, Chen G, Fan J. Synergistic effect of PARP inhibitor and BRD4 inhibitor in multiple models of ovarian cancer. J Cell Mol Med. 2023;27:634-49.
[15] Fard SS, Kouchaki S, Salimian Z, Sotoudeh M, Mousavi AS, Alimoghaddam K, et al. Overexpression of Bromodomain and Extraterminal Domain is Associated with Progression, Metastasis and Unfavorable Outcomes: Highlighting Prognostic and Therapeutic Value of the BET Protein Family in Gastric Cancer. Anti-Cancer Agents in Medicinal Chemistry. 2023;23:794-806.
[16] Lu L, Chen Z, Lin X, Tian L, Su Q, An P, et al. Inhibition of BRD4 suppresses the malignancy of breast cancer cells via regulation of Snail. Cell Death & Differentiation. 2020;27:255-68.
[17] Tan Y, Wang L, Du Y, Liu X, Chen Z, Weng X, et al. Inhibition of BRD4

suppresses tumor growth in prostate cancer via the enhancement of FOXO1 expression. Int J Oncol. 2018;53:2503-17.
[18] Hu Y, Zhou J, Ye F, Xiong H, Peng L, Zheng Z, et al. BRD4 inhibitor inhibits colorectal cancer growth and metastasis. Int J Mol Sci. 2015;16:1928-48.
[19] Zhang J, Dulak AM, Hattersley MM, Willis BS, Nikkila J, Wang A, et al. BRD4 facilitates replication stress-induced DNA damage response. Oncogene. 2018;37:3763-77.
[20] Yin M, Guo Y, Hu R, Cai WL, Li Y, Pei S, et al. Potent BRD4 inhibitor suppresses cancer cell-macrophage interaction. Nat Commun. 2020;11:1833.
[21] Huang LE. Carrot and stick: HIF-alpha engages c-Myc in hypoxic adaptation. Cell Death Differ. 2008;15:672-7.
[22] Gordan JD, Thompson CB, Simon MC. HIF and c-Myc: sibling rivals for control of cancer cell metabolism and proliferation. Cancer Cell. 2007;12:108-13.
[23] Reyes-González JM, Vivas-Mejía PE. c-MYC and Epithelial Ovarian Cancer. Front Oncol. 2021;11:601512.
[24] Zuber J, Shi J, Wang E, Rappaport AR, Herrmann H, Sison EA, et al. RNAi screen identifies Brd4 as a therapeutic target in acute myeloid leukaemia. Nature. 2011;478:524-8.
[25] Wang R, Yang JF, Ho F, Robertson ES, You J. Bromodomain-Containing Protein BRD4 Is Hyperphosphorylated in Mitosis. Cancers (Basel). 2020;12.
[26] Alsarraj J, Hunter KW. Bromodomain-Containing Protein 4: A Dynamic Regulator of Breast Cancer Metastasis through Modulation of the Extracellular Matrix. Int J Breast Cancer. 2012;2012:670632.
[27] Bretones G, Delgado MD, León J. Myc and cell cycle control. Biochim Biophys Acta. 2015;1849:506-16.
[28] Harper JW, Adami GR, Wei N, Keyomarsi K, Elledge SJ. The p21 Cdk-interacting protein Cip1 is a potent inhibitor of G1 cyclin-dependent kinases. Cell. 1993;75:805-16.
[29] Polyak K, Kato JY, Solomon MJ, Sherr CJ, Massague J, Roberts JM, et al. p27Kip1, a cyclin-Cdk inhibitor, links transforming growth factor-beta and contact inhibition to cell cycle arrest. Genes Dev. 1994;8:9-22.
[30] Schmider-Ross A, Pirsig O, Gottschalk E, Denkert C, Lichtenegger W, Reles A. Cyclin-dependent kinase inhibitors CIP1 (p21) and KIP1 (p27) in ovarian cancer. J Cancer Res Clin Oncol. 2006;132:163-70.
[31] Fu Y, Yang B, Cui Y, Hu X, Li X, Lu F, et al. BRD4 inhibition impairs DNA mismatch repair, induces mismatch repair mutation signatures and creates therapeutic vulnerability to immune checkpoint blockade in MMR-proficient tumors. Journal for ImmunoTherapy of Cancer. 2023;11:e006070.
[32] Rhyasen GW, Yao Y, Zhang J, Dulak A, Castriotta L, Jacques K, et al. BRD4 amplification facilitates an oncogenic gene expression program in high-grade serous ovarian cancer and confers sensitivity to BET inhibitors. PLoS One. 2018;13:e0200826.
[33] Chetry M, Bhandari A, Lin Y. Prognostic role of overexpressed Bromodomain and extra-terminal family in ovarian cancer. J Cancer. 2022;13:1695-705.
[34] Alqahtani A, Choucair K, Ashraf M, Hammouda DM, Alloghbi A, Khan T,

et al. Bromodomain and extra-terminal motif inhibitors: a review of preclinical and clinical advances in cancer therapy. Future Sci OA. 2019;5:Fso372.
[35] Beaufort CM, Helmijr JC, Piskorz AM, Hoogstraat M, Ruigrok-Ritstier K, Besselink N, et al. Ovarian cancer cell line panel (OCCP): clinical importance of in vitro morphological subtypes. PLoS One. 2014;9:e103988.
[36] Zhu P, Wang L, Xu P, Tan Q, Wang Y, Feng G, et al. GANT61 elevates chemosensitivity to cisplatin through regulating the Hedgehog, AMPK and cAMP pathways in ovarian cancer. Future Med Chem. 2022;14:479-500.
[37] Wilson AJ, Lalani AS, Wass E, Saskowski J, Khabele D. Romidepsin (FK228) combined with cisplatin stimulates DNA damage-induced cell death in ovarian cancer. Gynecol Oncol. 2012;127:579-86.
[38] Karakashev S, Zhang RG. Mouse models of epithelial ovarian cancer for preclinical studies. Zool Res. 2021;42:153-60.

# 초 록 (국문)

여성암에서 가장 예후가 나쁘다고 알려져 있는 난소암의 극복 방안으로 새로운 약제인 브로모도메인 함유 단백질(BRD) 4 저해제, OPT0139,의 항암효과와 기존 약제인 cisplatin과의 병합 사용 시의 부가효과를 확인하였다.

최근 10년 동안 여러 암종에서 후성유전학적 접근으로 항암 효과를 도모하려는 노력이 있어왔다. 그 중에서도 핵심 역할을 하는 BRD4에 관심이 집중되었지만, 난소암과 관련해서는 BRD4가 미치는 하위 경로를 이해하는 데에 한계가 있었다. 따라서 본 연구에서는 난소암 치료에서 신약인 OPT-0139의 항암 효과를 검증하고, 나아가 기존 치료제인 cisplatin과의 부가효과를 도모하고자 하였다.

실험 방법으로는 인간 난소암 세포의 마우스 이종이식 모델을 이용한 생체 내 연구를 수행하였고, 세포주는 난소암 세포주(SKOV3, OVCAR3)를 OPT-0139(1, 10 μM) ± 시스플라틴(10 μM)으로 48시간 동안 처리했다. 세포 생존력 및 증식은 MTT 및 ATP 분석, 세포 주기 정지 및 세포 사멸은 유세포 분석법을 사용하여 측정하였다. 실시간 중합효소연쇄반응(RT-PCR) 및 웨스턴 블롯팅을 사용하여 BRD4, c-Myc 및 세포사멸 관련 분자의 발현을 검출하였고, 이종이식 종양의 종양 성장률, 종양 무게 및 면역 조직 화학을 분석하여 통계분석을 시행하여 상피성 난소암에 대한 OPT-0139의 효과와 작용 기전을 확인하였다.

OPT-0139는 세포 생존율과 증식을 유의하게 감소시키고 세포사멸과 세포주기 정지를 유도한다. 마우스 이종이식 모델에서 종양의 성장, 부피, 무게 및 BRD4 관련 유전자 발현에 유의미한 변화가 관찰되어 BRD4 저해제 단독 사용 시의 항암 효과를 확인할 수 있었고, 시스플라틴과의 병합 요법은 단일 사용에 비해 세포 사멸을 촉진하고 시험관 및 생체 내에서 종양 성장을 더 억제했다.

이 연구 결과는 BRD4 저해제인 OPT-0139가 난소암에 대해 항암제로써

유망하다는 것을 보여준다. OPT-0139는 난소암에 있어서 세포 증식을 억제하고, 세포 생존력을 감소시키며, 세포 주기를 정지시키고, 세포 사멸을 유도한다. 이는 *in vitro*와 *in vivo* 실험을 통해 확인하였으며, 시스플라틴과의 병합 요법이 각각의 약제 단독 사용보다 모든 실험 결과에서 더 나은 항암 치료 효과를 보여주었다. 따라서 OPT-0139는 단독 또는 시스플라틴과 병용하여 사용한다면, 난소암을 치료하는 데 유망한 옵션이 될 수 있을 것으로 보인다.

**주요어 :** 난소암, BRD4 저해제, 항암효과
**학 번 :** 2021-39572